Original Article

Bone marrow-derived mesenchymal stem cells transplantation ameliorates renal injury through anti-fibrotic and anti-inflammatory effects in chronic experimental renovascular disease

Aline Almeida[*], *Rafaelle Lira, Mariana Oliveira, Marcela Martins, Yanca Azevedo, Karina R. Silva, Simone Carvalho, Erika Cortez, Ana Carolina Stumbo, Lais Carvalho, Alessandra Thole*

Laboratory of Stem Cell Research, Histology and Embryology Department, Biology Institute, State University of Rio de Janeiro, Rio de Janeiro, Brazil

ABSTRACT

Background: Progressive renal fibrosis is an underlying pathological process of chronic kidney disease (CKD) evolution. This study aimed to evaluate the roles of bone-marrow-derived mesenchymal stem cells (MSC) in the remodeling of fibrotic kidney parenchyma in the two kidneys-one clip (2K1C) CKD animal model.
Methods: Wistar rats were allocated into three groups: Sham, 2K1C, and 2K1C þ MSC. MSCs (106) were transplanted into the renal subcapsular region two weeks after clipping the left renal artery. Six weeks after clipping, left kidney samples were analyzed using histological and western blotting techniques. ANOVA tests were performed and differences between groups were considered statistically significant if $p < 0.05$.
Results: Clipped kidneys of 2K1C rats displayed renal fibrosis, with excessive collagen deposition, glomerulosclerosis and renal basement membrane disruption. Clipped kidneys of 2K1C þ MSC rats showed preserved Bowman's capsule and tubular basement membranes, medullary tubules morphological reconstitution and reduced collagen deposits. Expression levels of matrix metalloproteinase (MMP)-2 and MMP-9 were elevated, whereas tissue inhibitor of MMPs (TIMP)-1 and TIMP-2 levels were decreased in clipped kidneys of 2K1C rats. MSCs transplantation restored these expression levels. Moreover, MSCs suppressed macrophages and myofibroblasts accumulation, as well as TNF-a expression in clipped kidneys of 2K1C animals. MSCs transplantation significantly increased IL-10 expression.
Conclusions: Transplanted MSCs orchestrate anti-fibrotic and anti-inflammatory events, which reverse renal fibrosis and promote renal morphological restoration. This study supports the notion that only one MSCs delivery into the renal subcapsular region represents a possible therapeutic strategy against renal fibrosis for CKD treatment.

* *Corresponding author.* Laboratory of Stem Cell Research, Histology and Embryology Department, Biology Institute, State University of Rio de Janeiro, Boulevard Prof. Manoel de Abreu 444, 3_ Floor, 20550-170 Rio de Janeiro, RJ, Brazil.
   E-mail address: aline.aalmeida15@gmail.com (A. Almeida).

Chronic kidney disease (CKD) is a worldwide public health problem, which can progress to kidney failure [1] and the need for dialysis or even kidney transplantation. Progressive fibrosis of renal parenchyma is regarded as an underlying pathological process of CKD evolution [2,3], and it is commonly associated with infiltration of inflammatory cells, tubular atrophy, fibroblasts/myofibroblasts accumulation and aberrant extracellular matrix (ECM) deposition, mainly composed by collagens. An imbalance between matrix metalloproteinases (MMPs) and tissue inhibitors of matrix metalloproteinases (TIMPs) leads to uncontrolled proteolytic activity and has been implicated in renovascular fibrosis [4]. MMPs activity increases, particularly the gelatinases MMP-2 and MMP-9, promoting renal fibrosis development by collagen IV degradation in the renal basement membrane, a process that triggers tubular epithelial transition towards a mesenchymal and fibrogenic phenotype, named epithelial–mesenchymal transition (EMT), which in turns contributes to increase myofibroblasts number and exacerbation of ECM components production [5,6]. The replacement of normal tissue by scar tissue leads to renal function loss, however, there are no efficient therapies to halt or reverse renal fibrosis [7,8].

Stem cell-based therapies have emerged as a regenerative approach to treat renal diseases, especially based on the use of mesenchymal stem cells (MSCs) [9]. MSCs can be easily isolated in clinical useful numbers from different tissue sources, like bone marrow and adipose tissue, and secrete a wide range of bioactive molecules like chemokines, cytokines, and growth factors that can mediate anti-scarring and regenerative processes, besides immune regulation [10,11]. Our group and others have previously demonstrated that bone marrow-derived MSCs transplantation reduces renal fibrosis and improves the function of ischemic kidney in two-kidney, one-clip (2K1C) CKD preclinical model by reduction of proteinuria

and urea concentration, increase of protein plasma levels, and a tendency to reduce creatinine [12,13].

In 2K1C model, partial occlusion of the renal artery (stenosis) leads to reduced blood flow and perfusion pressure, causing renovascular hypertension (RVH), a disease regarded as a secondary hypertension form in humans [14]. Renal artery stenosis activates the renin–angiotensin–aldosterone system (RAAS), promoting oxidative stress, inflammation, microvascular loss, severe interstitial fibrosis and tubular atrophy, resulting in functional kidney deterioration [12,13] and further progress to CKD and renal failure [15]. We have recently shown that MSC renal subcapsular administration led to a significant reduction in blood pressure arguing a strong effect on renin release by actions on juxtaglomerular apparatus. Moreover, GFP$^+$ MSCs were detected throughout the entire kidney, near to inflammatory cell infiltration and in fibrotic areas [12]. However, the mechanisms by which MSCs reverse tissue fibrosis, regenerate renal parenchyma and improve renal function in renal artery stenosis induced-CKD models are not fully understood. Considering the immunosuppressive and regenerative properties of MSCs, we hypothesized that these cells could have a key role in orchestrating fibrotic clipped kidney parenchyma remodeling by targeting and modulating the resident cell types involved in inflammatory and fibrogenic events, as well as the expression of inflammatory and tissue remodeling mediators. Therefore, in the present study, we aimed to determine whether MSCs transplantation could modulate the presence of macrophages and myofibroblasts, and the expression of tumor necrosis factor-α (TNF-α) and interleukin-10 (IL-10) in clipped kidneys of 2K1C rats. The expression pattern of the tissue remodeling proteins MMP-2, MMP-9 and its respectively inhibitors TIMP-2 and TIMP-1, was also investigated.

Material and Methods

Two kidneys-one clip (2K1C) animal model and experimental groups

Male Wistar rats (2 months old) were kept in a temperature-controlled environment (21 ± 2 °C), with inverted light cycles (h–h light–dark), fed with commercial feed (Nuvilab, Brazil) and filtered water, both ad libitum.

The model of two kidneys-one clip (2K1C) established by Goldblatt et al. [16] was used in this study to induce renal fibrosis by renal artery stenosis in rats. Surgical procedures were performed as previously described [12,17]. Briefly, rats were put under ketamine and xylazine anesthesia (100 and 5 mg kg^{-1}, respectively, I.P. injection) and underwent surgery for partial occlusion of the left renal artery with the aid of a 0.2 mm silver clip. The 2K1C rats were divided into two groups (n = 6 for each group): the 2K1C group (n = 6) and the 2K1C + MSCs (n = 6), which received 10^6 bone marrow-derived MSCs injected into the subcapsular region of the clipped kidney, once, four weeks after the clipping surgery, when renal artery stenosis-induced fibrosis was already established [16,17]. Animals were euthanized six weeks after the clipping procedure. A control group (Sham, n = 6) was established with animals that underwent surgical intervention that omits the step of renal artery occlusion. Renal functional parameters

(proteinuria, plasma creatinine, urea concentration, urinary protein excretion) and systolic blood pressure (SBP) were assessed weekly as previously described [12], in order to confirm the expected renal functional disturbances and the establishment of hypertension in 2K1C animals.

The experimental groups were euthanized six weeks after the clipping procedure. The left kidney (clipped) of all animals was collected and divided into fragments containing both cortical and medullary regions for morphological and protein expression evaluation. All animals used in this study underwent procedures previously approved by the Ethics Committee in Animal Experimentation of the State University of Rio de Janeiro (registered under CEUA/062/20) and in accordance with the standard guidelines on animal experimentation of the Brazilian National Council of Animal Experimentation Control (CONCEA). Data regarding renal functional parameters after clipping and MSC transplantation procedures have been published in a previous study [12].

MSCs isolation, culture and transplantation

Bone marrow derived MSCs were obtained from femurs and tibias of male *Wistar* rats (two months old) euthanized in a CO_2 chamber as previously described [12]. Briefly, bone medullary cavities were exposed and harvested by centrifugation at 350g for 10 min. Bone marrow mononuclear cells were obtained by Ficoll-Hypaque (Sigma–Aldrich, St Louis, MO, USA) density gradient, plated in 25 cm^2 culture flasks and maintained in high-glucose Dulbecco's modified Eagle's medium (DMEM; Sigma–Aldrich), pH 7.2, supplemented with 20% fetal bovine serum (Cultilab, Campinas, SP, Brazil) and antibiotics until the monolayer of MSCs reached 80% confluence. Adherent cells were harvested from culture flasks with trypsin–EDTA 0,25% (Sigma–Aldrich), then subsequently cultured for further expansion up to the third passage to ensure a homogeneous MSC culture. Our group has already described the differentiation capacity and surface expression of the obtained MSCs [12].

For MSCs transplantation, cells at the third passage were harvested with Accutase cell detach medium (Thermo Fischer Scientific, Waltham, MA, USA), counted in the Neubauer chamber. Syringes were prepared with 10^6 MSCs suspended in 0.5 mL of phosphate buffered saline (PBS). MSCs injection was performed with a 31G needle into the subcapsular region of the clipped kidney of animals from the 2K1C + MSCs group.

Kidney histology

After euthanasia, a sample of the left kidney was collected, fixed with 10% buffered formaldehyde, dehydrated in crescent series of ethanol, diaphanized in xylol and embedded into paraffin. Tissue sections of 5 μm were stained for 1 h with 0,1% of Direct Red 80 (Picrosirius Red staining) and counterstained with hematoxylin, and with Masson's Trichrome stain [13, 16], for the observation of collagen fibers distribution. Basement membrane integrity was evaluated using Periodic acid–Schiff (PAS) staining method. Tissue sections were incubated for 5 min in periodic acid, washed in distilled water, stained for 10 min with Schiff reagent and counterstained with hematoxylin. Images of histological sections were acquired with an Olympus BX53 light microscope (Nagabo, Chubu, Japan),

equipped with a CCD camera (Olympus DP72). Picrosirius Red stained sections were evaluated under both non-polarized and polarized light.

Immunohistochemistry

Paraffin-embedded left kidneys sections were deparaffinized through xylene, hydrated with a decrescent series of ethanol, and incubated for 20 min with 3% hydrogen peroxide to block endogenous peroxidase activity. Antigen unmasking was done by incubating sections with citrate buffer (pH 6.0) at 60 °C. Unspecific binding of immunoglobulins was achieved by incubating sections with 2.5% normal horse serum from Vectastain® Universal Quick HRP Kit (Peroxidase, Vector Laboratories, Burlingame, CA, USA). Sections were then incubated overnight at 4 °C with polyclonal primary antibodies against the following proteins: anti-collagen IV (1:500 Santa Cruz, Dallas, TX, USA), anti-CD68 (1:200, Biogenesis, RS, Brazil), anti-α-SMA (1:200, Biorbyt, Cambridge, UK), anti-IL-10 (1:100, Biorbyt) and anti-TNF-α (1:100, Santa Cruz). Slides were further incubated with biotinylated universal secondary antibody, streptavidin-peroxidase (from VECTASTAIN® Universal Quick HRP Kit, Vector, Cambridge, UK) and 3,3-diaminobenzidine tetrahydrochloride (DAB) chromogen (DAB Peroxidase (HRP) Substrate Kit, Vector), according to the manufacturers' recommendations. Cells nuclei were stained with hematoxylin, and then, slides were dehydrated and mounted with Entellan (Merck, Germany). Sections were examined under an Olympus BX53 light microscope. The immunohistochemistry reaction was also carried out in the absence of the primary antibody as a control of non-specific secondary antibody binding. Three technical repetitions were performed for each target.

For staining quantifications, high-powered images (x400 magnification) of 20 randomly selected histological fields from each animal were acquired with a CCD camera (Olympus DP72) coupled to the light microscope. Quantification of collagen IV, CD68, α-SMA and IL-10 expression was performed by measuring the tissue area that reacted with the antibody, expressed as pixels/μm^2. All quantifications were performed using Image-Pro Plus 7.0 software (Media Cybernetics, Rockville, MD, USA).

Western blotting

Samples of the left kidneys collected from experimental groups (100 mg) were incubated with RIPA buffer (50 mM Tris, 30 mM sodium pyrophosphate, 150 mM NaCl, 1% Triton X-100, 0.1% SDS, 50 mM sodium fluoride, 1 mM sodium orthovanadate) containing a protease inhibitor cocktail (Roche, Basel, Switzerland). Samples were centrifuged at 10,640g for 30 min at 4 °C, the supernatant was collected and the protein concentration in samples were estimated using BCA protein assay kit (Thermo Fischer Scientific). Then, samples were solubilized in Laemmli sample buffer (50 mM Tris–HCl, pH 6.8, 10% glycerol, 5% 2 β-mercaptoetanol, 1% SDS, and 0.001 bromophenol blue) at 95 °C for 5 min and then kept at −20 °C. Proteins were added to 10% or % polyacrylamide gels for separation (1 h, 150v) along with pre-stained molecular weight standard (Full Range Rainbow; Amersham Biosciences, UK). After electrophoresis, proteins were transferred to nitrocellulose membranes (HybondP; Amersham) for 1 h at 15v. Membranes were blocked
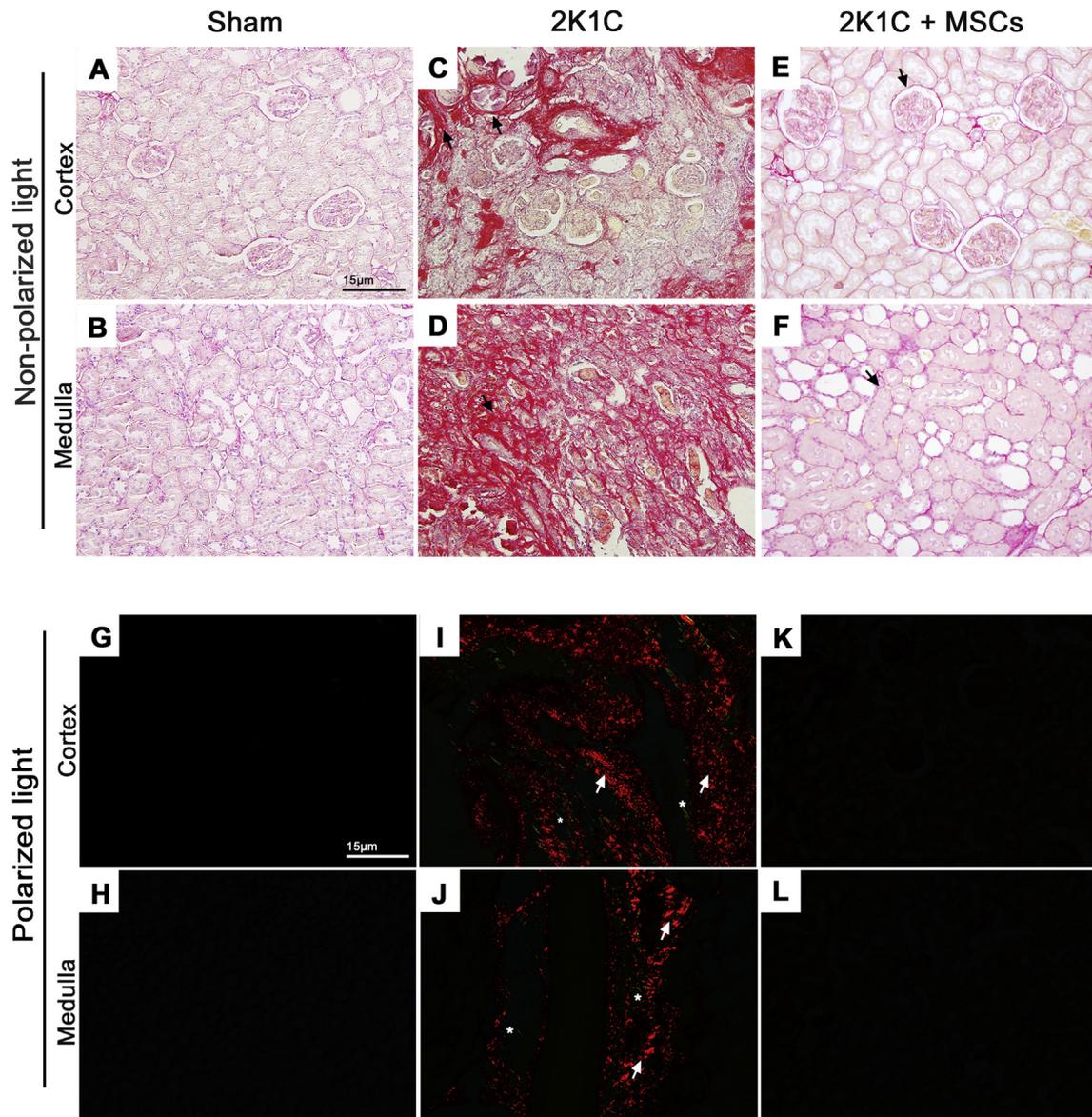
Fig. 1 **MSCs transplantation ameliorates fibrosis and renal tubulointerstitial injury in 2K1C rats.** Picrosirius red-stained left kidney sections of renal cortex and medulla examined under non-polarized (A–F) and polarized (G–L) light microscopy from sham, 2K1C and 2K1C + MSCs groups. Sham kidneys preserve regular histoarchitecture, with minimal interstitial space (A, B) and display no collagen birefringence under polarized light evaluation (G, H). An intense collagen deposition in a widened interstitial space was detected both in the cortex and medulla of 2K1C clipped kidneys (C, D, I, J). 2K1C + MSCs group displayed a normal renal parenchyma, with no collagen birefringence detection (K, L). Black arrows indicate areas with collagen localization stained in red. White arrows and asterisks indicate orange-red and yellow-green birefringence, respectively. Scale bars = 15 μm; 2K1C = Two Kidney-One Clip; MSCs = Mesenchymal Stem Cells.

with 5% non-fat dry milk in 0.05% Tween-TBS for 1 h and incubated overnight with the following primary antibodies: anti-MMP-2 and -9 (1:500), anti-TIMP-1 and -2 (1: 500), anti-TNF-α (1:200), anti-β-actin (1:1000) (all from Santa Cruz Biotechnology), anti-CD68 (1:1000, Abcam), and anti-ACTA2 (1:200, Biorbyt). Membranes were further incubated with biotinylated secondary antibody and streptavidin-peroxidase (1:5000 and 1:10,000 in Tween-Tris Buffered Saline, respectively. Invitrogen, Carlsbad, CA, US). Finally, membranes were incubated with chemiluminescence substrate (Amersham ECL prime, GE Healthcare, Chicago, IL, US) and revealed in ChemiDoc MP

(BioRad, Hercules, CA, EUA). Four technical repetitions were performed for each target.

Immunoreactive bands densitometry was performed by Adobe Photoshop Elements 9 software on images obtained by Image Lab software (BioRad). All proteins band densities were normalized to β-actin internal control during analysis.

Statistical analysis

To assess statistical differences among the experimental groups evaluated by immunohistochemistry and western blotting,
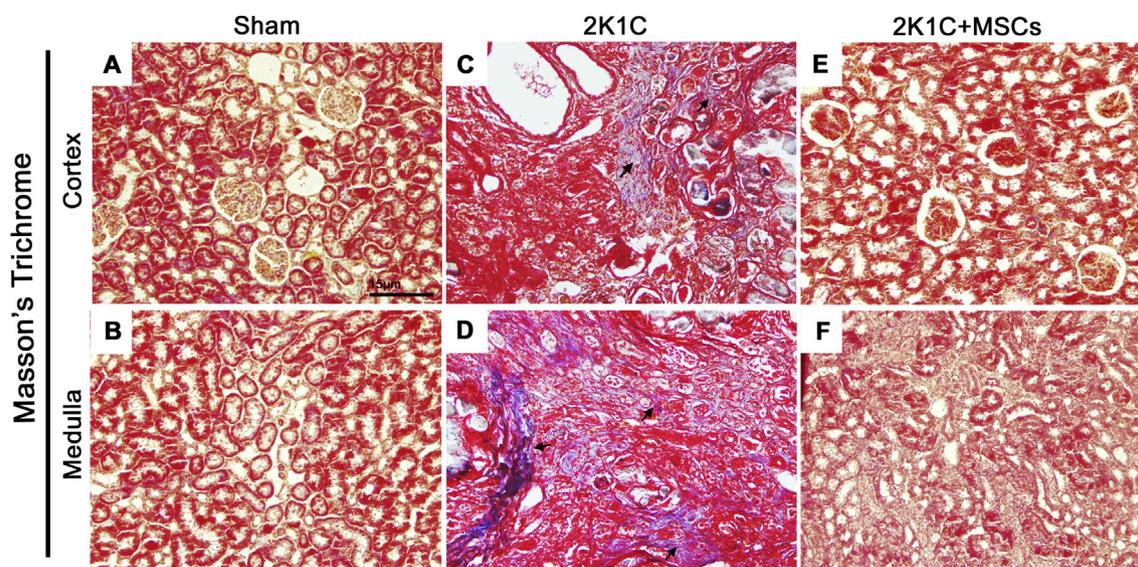
Fig. 2 **MSCs transplantation ameliorates collagen deposition in clipped kidneys of 2K1C rats.** Masson Trichrome-stained left kidney sections of renal cortex and medulla from sham (A, B), 2K1C (C, D) and 2K1C + MSCs (e, f) groups. Sham kidneys display no detectable collagen deposition (A, B). An intense collagen deposition in the interstitium was detected both in the cortex and medulla of 2K1C clipped kidneys (C, D). No collagen deposition was detected in the renal tissue of clipped kidneys from 2K1C + MSCs group (E, F). Black arrows indicate areas with collagen deposition stained in blue. Scale bars = 15 μm; 2K1C = Two Kidney-One Clip; MSCs = Mesenchymal Stem Cells.

parametric and unpaired one-way ANOVA tests were performed followed by Tukey's post-test for multiple comparisons. Tests were performed using the software GraphPad Prism 5 (GraphPad Prism Inc., La Jolla, CA, US). Results are presented as mean ± standard error (SE) and $p < 0.05$ was considered statistically significant.

Results

MSCs transplantation attenuates fibrosis and promotes basement membrane structural regeneration in clipped kidneys

Collagen accumulation in Sham and 2K1C-clipped kidneys was detected using Picrosirius Red and Masson's Trichrome stainings [Figs. 1 and 2, respectively]. Development of a fibrotic injury was confirmed in clipped kidneys, characterized by an intense collagen deposition between renal corpuscles (cortex) and through the tubulointerstitium (medulla) after six weeks of renal artery stenosis [Fig. 1C and D; Fig. 2C and D], which was not observed in Sham group [Fig. 1A and B; Fig. 2A and B]. Evaluation of picrosirius red-stained sections under polarized light also revealed a widespread accumulation of collagen in the clipped kidney of 2K1C group, with a predominance of orange-red over yellow-green birefringence [Fig. 1I and J], while no refringence was observed in the renal tissue of Sham group [Fig. 1G and H]. However, tissue fibrosis strikingly reduced after 2 weeks of MSCs transplantation, together with renal parenchyma improvement and corpuscles, tubules and tubular lumen recovery [Fig. 1E, F, K, L; Fig. 2E and F].

Renal artery stenosis in the 2K1C rats have led to basement membrane disruption of the parietal layer of Bowman's capsule and tubules, as indicated by PAS staining, besides loss of tubule integrity [Fig. 3C and D]. Although 2K1C group has shown an elevated expression of collagen IV, it was dispersed throughout the renal cortex and the medullary interstitium [Fig. 3I and J] instead of restricted to basement membrane [Fig. 3G and H]. Renal artery stenosis in 2K1C rats resulted in a 4-fold increase of collagen IV deposition in the clipped kidney compared with kidneys from the Sham group [Fig. 3M, $p < 0.0001$]. Conversely, 2K1C + MSCs group showed preserved Bowman's capsule and tubular basement membranes besides medullary tubules reconstitution [Fig. 3E and F]. Collagen IV expression was reduced [Fig. 3K—M $p < 0.0001$ vs 2K1C] to levels comparable to the Sham group, mainly restricted to basement membranes [Fig. 3M - $p > 0.05$].

MMPs and TIMPs expression levels are restored after MSCs transplantation in clipped kidneys

Aiming to investigate the mechanisms by which MSCs transplantation ameliorated the ECM accumulation in renal tissue of 2K1C rats, a quantitative analysis of MMP-2 and -9 expression, as well as of its inhibitors TIMP-1 and -2, was performed using western blotting [Fig. 4]. It was observed an increase of MMP-2 and -9 expression [Fig. 4A and B - black bars — $p < 0.001$ and $p < 0.05$, respectively] and a decrease of TIMP-1 and -2 expression [Fig. 4C and D — black bars — $p < 0.0001$] in clipped kidneys compared to Sham group. Conversely, disturbances were not observed in 2K1C + MSCs group, neither for MMPs [Fig. 4A and B - gray bars — $p < 0.05$ vs 2K1C group] nor for TIMPs expression [Fig. 4C and D — gray bars - $p < 0.0001$ vs 2K1C group], which showed expression levels similar to Sham group [Fig. 4 - white bars, $p > 0.05$ vs Sham].
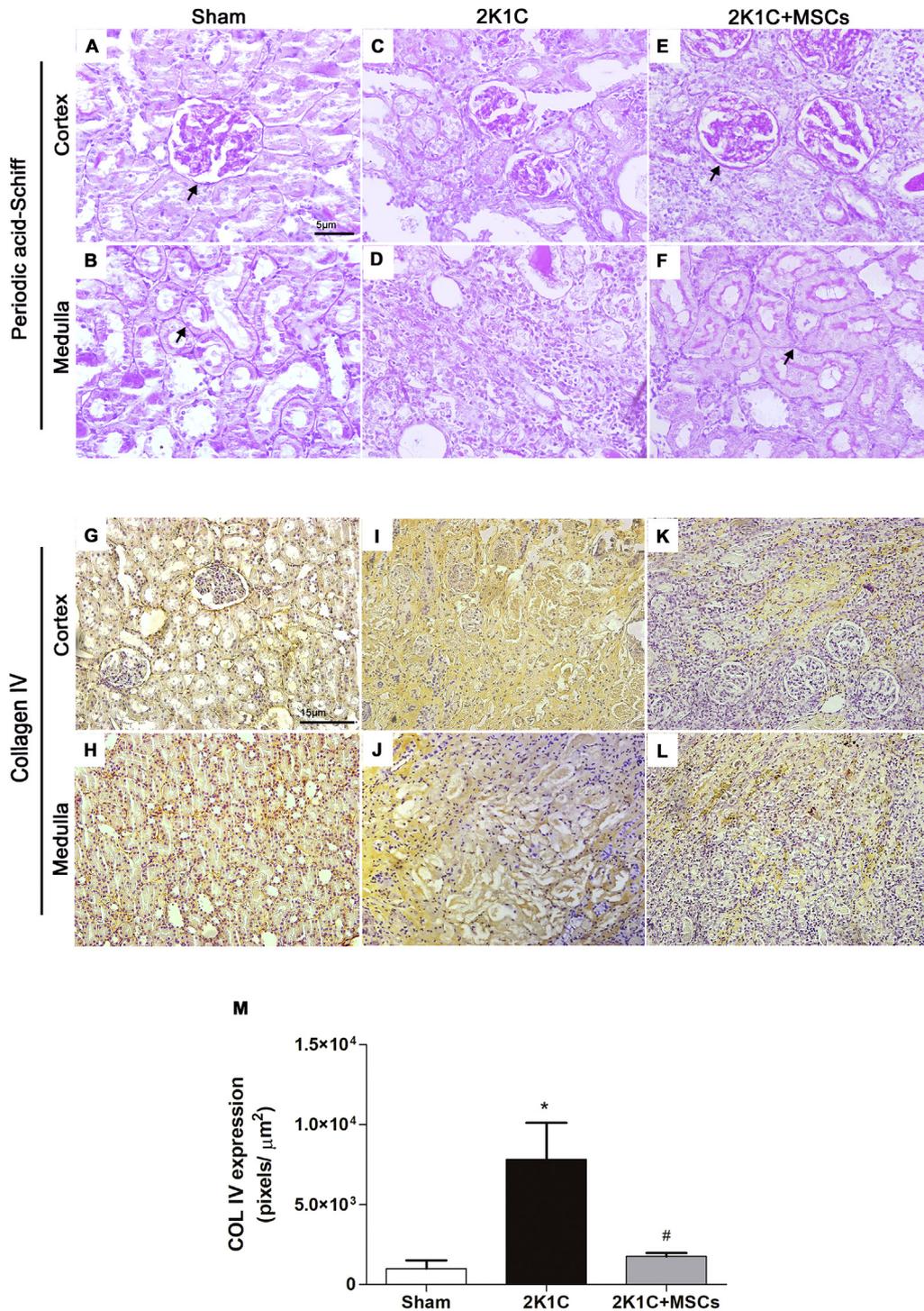
Fig. 3 **MSCs transplantation promotes regeneration of basement membranes and reduce collagen IV accumulation in clipped kidneys.** Representative photomicrographs of renal cortex and medulla histological sections stained by the PAS method (A–F) and immunolabeled with anti-collagen IV (G–L). Renal cortex and medulla of Sham group maintains the regular structural integrity of basement membranes (A, B) with collagen IV staining around Bowman's capsule and tubules (G, H). The basement membrane was poorly defined in 2K1C clipped kidney sections (C, D), while collagen IV was intensively detected dispersed throughout the parenchyma (I, J). Both the cortex and the medulla of 2K1C + MSCs group display a structured basement membrane around Bowman's capsule and tubules (E, F), and reduced collagen IV stained areas (K, L) compared to 2K1C untreated group. Arrows indicate the basement membrane. (M) Semi-quantitative analysis of collagen IV expression. Values are represented as means ± SE (n = 6). ANOVA test resulted in $p < 0.0001$. Post-test results: *$p < 0.001$ vs. SHAM. #$p < 0.05$ vs. 2K1C. Scale bars: (A–F) 5 μm; (G–L) 15 μm; 2K1C = Two Kidney-One Clip; MSCs = Mesenchymal Stem Cells.
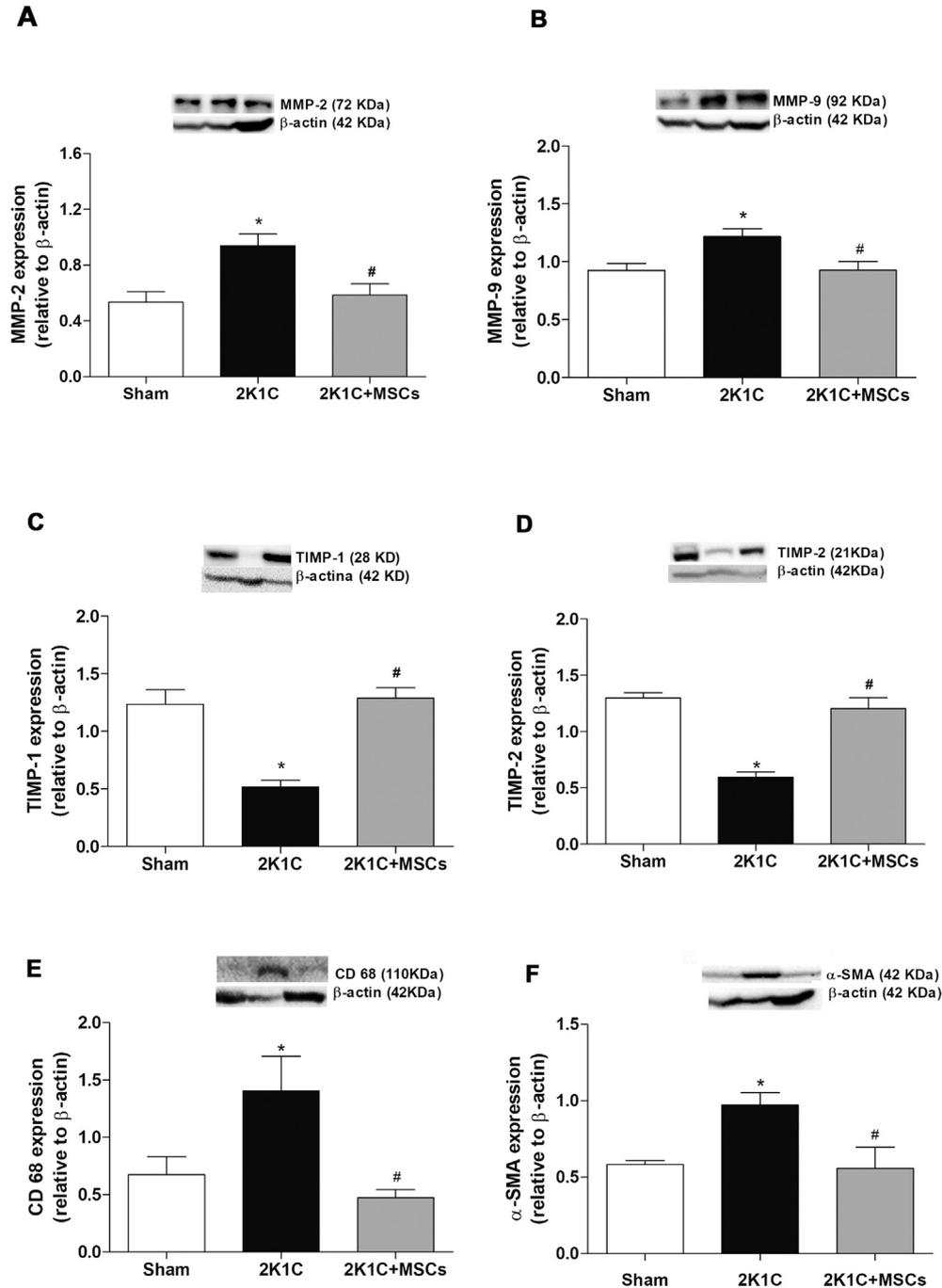
Fig. 4 **MSCs transplantation restores MMPs, TIMPs, α-SMA and CD68 expression levels in clipped kidneys.** Western blotting analysis of MMP-2 (A), MMP-9 (B), TIMP-1 (C), TIMP-2 (D), CD-68 (E), α-SMA (F) expression in the left kidney of sham, 2K1C and 2K1C + MSCs groups. Graphs show protein levels normalized to β-actin expression. 2K1C clipped kidneys displayed an increase in MMPs, CD-68 and α-SMA (A, B, E, F − black bars) and a decrease in TIMPs (C, D − black bars) expression compared to sham group (white bars). 2K1C + MSCs group showed levels of MMPs (A, B − gray bars), TIMPs (C, D − gray bars), CD68 (e-gray bars) and α-SMA (f-gray bars) similar to sham group. Values are represented as means ± SE (n = 6). ANOVA test resulted in $p = 0.0050$ (A), $p = 0.0113$ (B); $p < 0.0001$ (C, D), $p = 0.0169$ (E), $p = 0.0215$ (F). Post-test results: $*p < 0.001$, $p < 0.05$, $p < 0.0001$, $p < 0.0001$, $p < 0.05$, $p < 0.05$ vs. Sham (A, B, C, D, E, F, respectively); $\#p < 0.05$, $p < 0.05$, $p < 0.0001$, $p < 0.0001$, $p < 0.05$, $p < 0.05$ vs. 2K1C (A, B, C, D, E, F, respectively). 2K1C = Two Kidney-One Clip; MSCs = Mesenchymal Stem Cells.
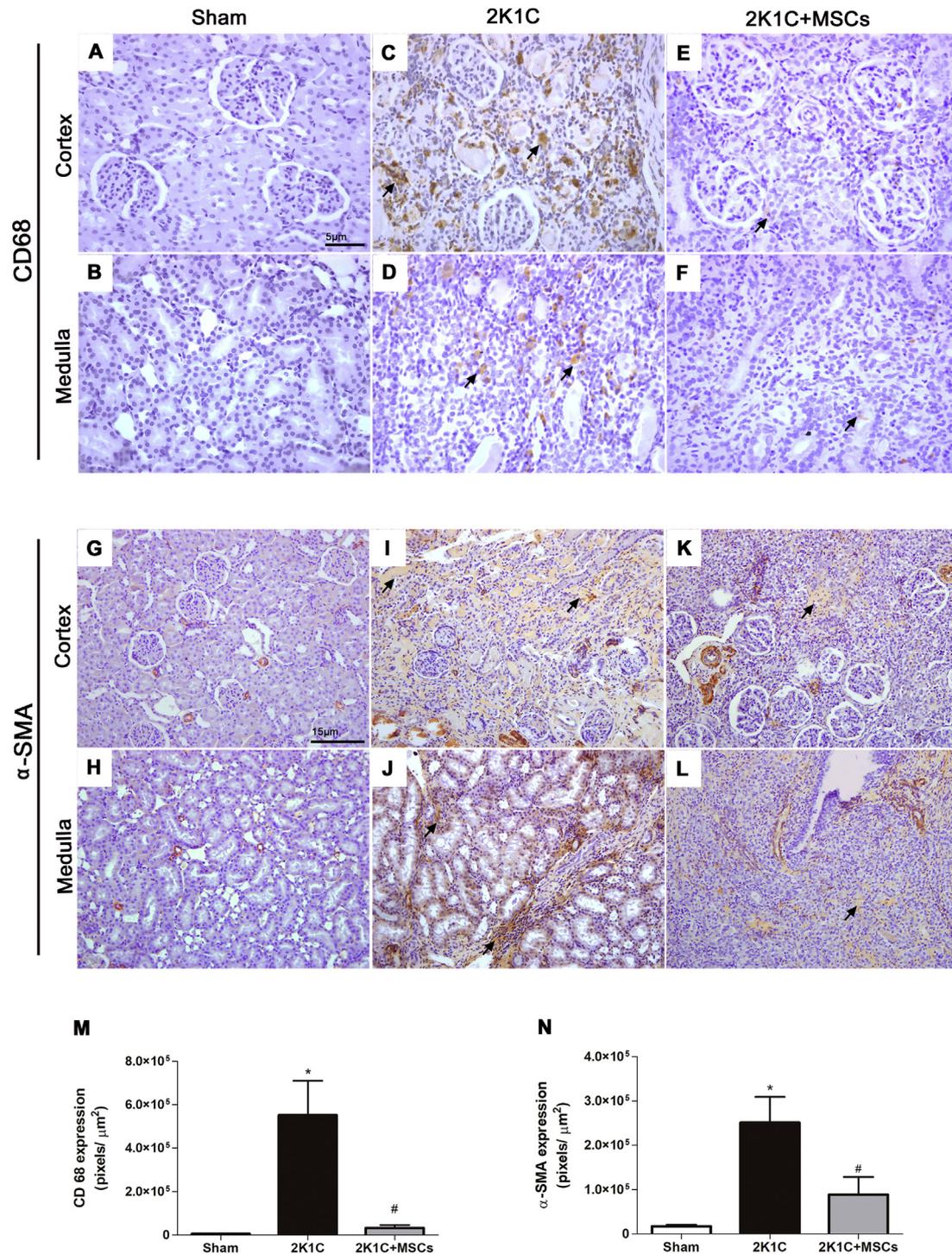
Fig. 5 **MSCs transplantation suppressed macrophage and myofibroblast accumulation in clipped kidneys.** Representative micrographs of left kidney sections immunolabeled with anti-CD68 (A−F) and anti-α-SMA (H−M) to identify macrophages and myofibroblasts, respectively. Sham-left kidney displayed no macrophage staining (A, B) and some α-SMA-positive areas within smooth-muscle arterioles (G, H). Clipped kidneys from the 2K1C group showed an intense staining for both cell types throughout the cortex parenchyma and the tubulointerstitial area (C, D, I, J). 2K1C + MSCs group displayed less renal areas stained for macrophages (E, F) and myofibroblasts (K, L) than 2K1C group. Scale bars: 15 μm. Black arrows indicate stained areas. (M, N) Semi-quantitative analysis of the CD68 and α-SMA expression. Values are represented as means ± SE (n = 6). (M) ANOVA test resulted in $p = 0.0018$. Post-test results: *$p < 0.001$ vs Sham; #$p < 0.0001$ vs 2K1C. (N) ANOVA test resulted in $p = 0.004$. Post-test results: *$p < 0.001$ vs Sham; #$p < 0.05$ vs 2K1C. 2K1C = Two Kidney-One Clip; MSCs = Mesenchymal Stem Cells.
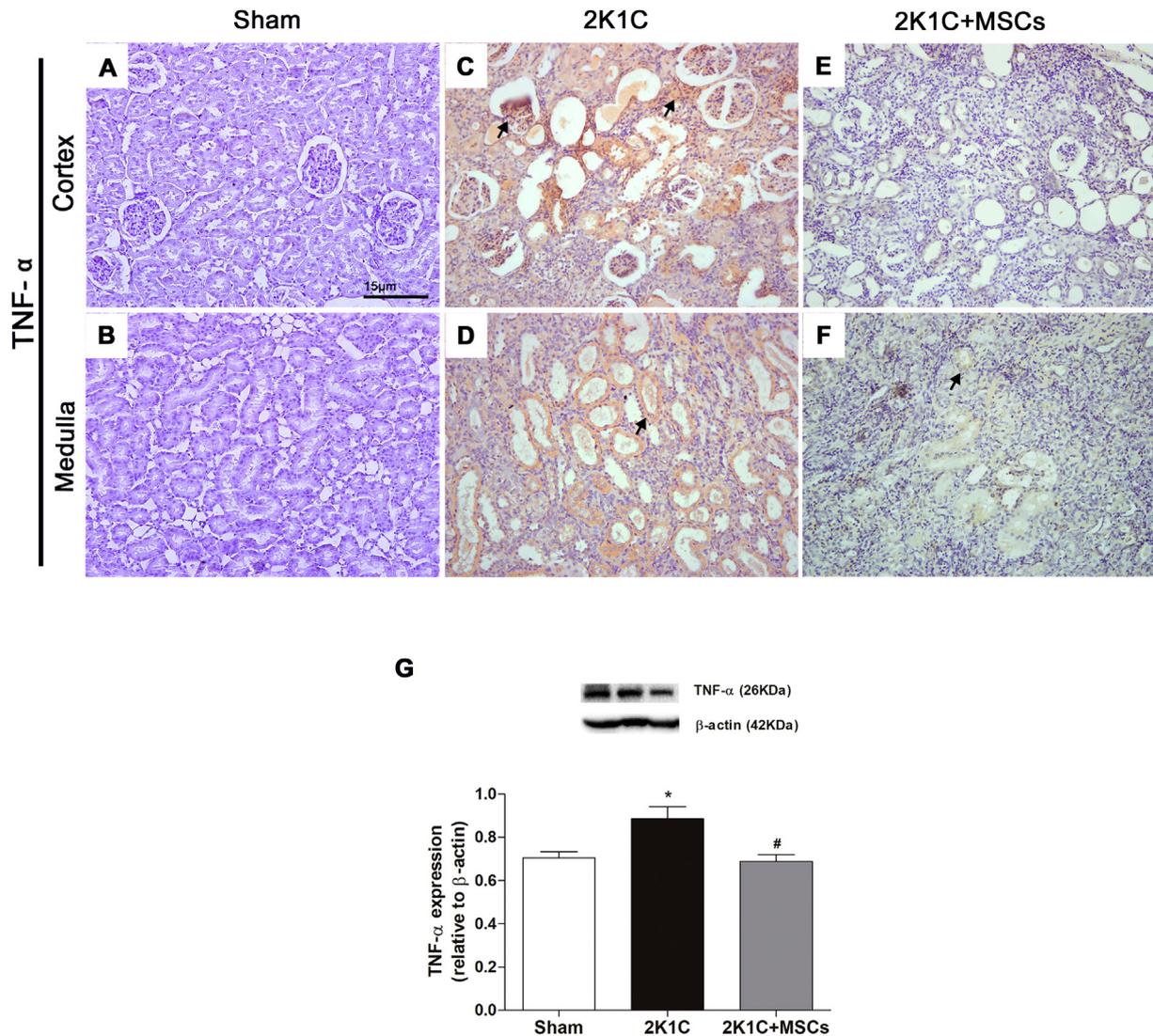
Fig. 6 **TNF-α increase in clipped kidneys was suppressed after MSCs transplantation.** Representative micrographs of left-kidney sections immunolabeled with anti-TNF-α (A–F). Sham kidney showed scarce staining for TNF-α (A, B). Clipped kidney from the 2K1C group showed an intense staining for TNF-α both in the cortex parenchyma (C) and around medullary tubules (D). 2K1C + MSCs group displayed less TNF-α stained areas (E, F) than 2K1C group. Scale bars: 15 μm. Black arrows indicate stained areas. (G) Western blotting analysis of TNF-α expression. Graph shows protein levels normalized to β-actin expression. Values are represented as means ± SE (n = 6). ANOVA test resulted in $p = 0.03$. Post-test results: *$p < 0.05$ vs. SHAM. #$p < 0.05$ vs. 2K1C. 2K1C = Two Kidney-One Clip; MSCs = Mesenchymal Stem Cells.

MSCs transplantation suppressed macrophage and myofibroblast accumulation in clipped kidneys

CD68 and α-SMA expression was examined by western blotting [Fig. 4E and F] and immunohistochemistry [Fig. 5] to evaluate monocyte/macrophage infiltration and the presence of myofibroblasts in clipped kidneys. Protein expression evaluated by western blotting showed an increase of CD68 and α-SMA expression [Fig. 4E and F - black bars - $p < 0.05$ vs Sham group] in clipped kidneys compared to Sham group, and a decrease of these proteins in the 2K1C + MSCs group [Fig. 4E and F - gray bars - $p < 0.05$ vs 2K1C group] compared to 2K1C group, to levels similar to Sham group. While no CD68 staining

was observed in Sham group using immunohistochemistry [Fig. 5A and B], CD68+ cells were detected both in the cortex and medulla from renal artery stenosis-induced injured kidneys [Fig. 5C and D], showing a remarkable increase in the stained area of 2K1C group [Fig. 5M, $p \leq 0.0001$ vs. Sham]. However, this accumulation was not observed in 2K1C + MSCs group, which showed scarce CD68+ cells [Fig. 5E and F] with a stained area significantly smaller than 2K1C group [Fig. 5M, $p \leq 0.0001$] and similar to Sham group [Fig. 5G, $p > 0.05$].

The marker of myofibroblast differentiation, α-SMA, was located within arterioles of Sham left kidneys [Fig. 5G and H]. However, clipped kidneys of 2K1C group showed a significant increase of myofibroblast population, with α-SMA expression
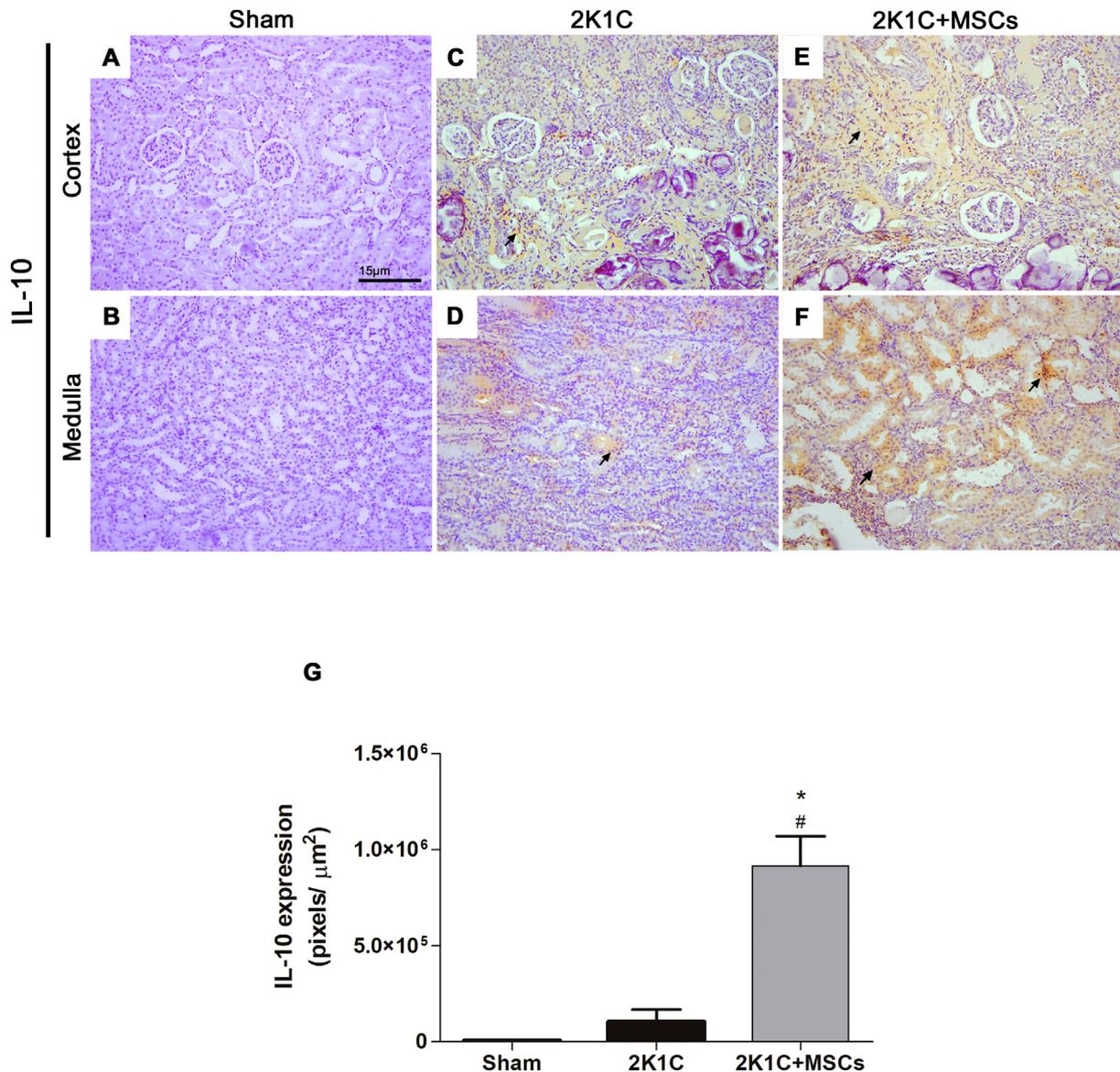
Fig. 7 **MSCs transplantation increases IL-10 expression in clipped kidneys.** Representative micrographs of kidneys sections immunolabeled with anti-IL-10 (A–F). Sham kidney showed no staining for IL-10 (A, B). Clipped kidney from the 2K1C group showed a light staining for IL-10 both in the cortex parenchyma (C) and around medullary tubules (D). 2K1C + MSCs group displayed a higher intensity of IL-10 staining (E, F) than 2K1C group (C, D). Scale bars: 15 μm. Black arrows indicate stained areas (n = 6). (G) Semiquantitative analysis of IL-10 expression. Values are represented as means ± SE. ANOVA test resulted in $p < 0.0001$. Post-test results: *$p < 0.0001$ vs Sham; #$p < 0.0001$ vs 2K1C. 2K1C = Two Kidney-One Clip; MSCs = Mesenchymal Stem Cells.

found throughout the cortex parenchyma and the tubulointerstitial area [Fig. 5I, J, N - $p \leq 0.0001$ vs. Sham]. Conversely, MSCs injection in clipped kidneys induced a significant decrease in myofibroblast accumulation when compared to 2K1C group [Fig. 5K, L, N − $p < 0.05$], to levels with no statistical differences from Sham group [Fig. 5N, $p > 0.05$].

MSCs transplantation has opposite effects on TNF-α and IL-10 expression in clipped kidneys

In order to investigate the expression pattern of immune mediators in renal tissue of the experimental groups, the expression of TNF-α and IL-10 (pro- and anti-inflammatory cytokines, respectively) was evaluated.

No expression of TNF-α [Fig. 6A and B] and IL-10 [Fig. 7A and B] were detected by immunohistochemistry in clipped kidney sections of Sham group. Conversely, a significant upregulation of TNF-α expression was achieved both in the renal cortex and medulla of 2K1C group [Fig. 6C, D, G, $p < 0.05$ vs. Sham]. A slight signal of IL-10 expression was detected in the renal tissue of the clipped kidneys from 2K1C animals [Fig. 7C and D], which was not statistically different from Sham group [Fig. 7G, $p > 0.05$]. Notably, while MSCs transplantation significantly suppressed the TNF-α increase [Fig. 6E–G, $p < 0.05$ vs. 2K1C] to levels similar to those found in Sham group [Fig. 6G, $p > 0.05$ vs. Sham], it promoted a strong upregulation (nine-fold) of IL-10 expression in 2K1C rats [Fig. 7E–G, $p < 0.0001$ vs. 2K1C]. Interestingly, IL-10 expression of the 2K1C + MSCs group was also significantly higher than the expression found in Sham group [Fig. 7G, $p < 0.0001$].

Discussion

This study demonstrated that bone marrow-derived MSCs delivery into the renal subcapsular area ameliorates renal fibrosis in 2K1C rats, as evidenced by a striking reduction of collagen deposition, Bowman's capsule and tubulointerstitial basal membranes morphological recovery, a significant suppression of myofibroblast and macrophage accumulation, as well as a reduction of TNF-α, and increase in IL-10 expression. Moreover, this is the first study to report the restorative effects of local administration of MSCs on the balance between MMP-2/MMP-9 and TIMP-1/TIMP-2 expression in clipped kidneys of 2K1C rats. These results indicate that MSCs have a therapeutic potential for the renal artery stenosis consequences and CKD through immunomodulatory and antifibrotic effects, which lead to structural repair and tissue remodeling.

The delivery of stem cells at the renal subcapsular region of the clipped kidney allows a great number of cells to home in and interact for a long time with the injured site [18,16]. Therefore, in this study, the subcapsular administration route of stem cells was chosen to analyze the local effects of MSC transplantation in the fibrogenic environment of kidneys damaged by renal artery stenosis.

Renal artery stenosis develops interstitial fibrosis, tubular epithelial injury, in addition to loss of peritubular capillaries and infiltration of pro-inflammatory macrophages [19]. The 2K1C experimental model is dependent on the activation of RAAS. Angiotensin II promotes renal fibrosis by stimulating the synthesis of TGF-β by renal cells [20], a pro-fibrotic factor that promotes the activation of fibroblasts into myofibroblasts, which produce large amounts of ECM components, mainly collagen [20–22]. This triggers fibrosis in the kidney, promoting deterioration of kidney function, and increasing kidney damage [22]. Due to the proteolytic ability of MMPs, they are commonly considered to degrade and reduce excessive ECM accumulation, thereby decreasing renal fibrosis after injury [23]. However, evidences suggest that MMP-2 and MMP-9 activity increases after renal damage, leading to the degradation of renal basement membranes, contributing to EMT, a feature of renal fibrosis, which could also contribute to rise myofibroblasts number in the injured kidney [5,6]. Accordingly, in the present study, 2K1C rats showed upregulated

MMP-2 and MMP-9 expression and downregulated TIMP-1 and TIMP-2 expression in comparison to Sham, along with disruption of Bowman's capsule and tubular basement membranes, collagen IV and total collagen overproduction, and increased myofibroblast population in clipped kidneys.

There is a clear relationship between the pro-fibrotic TGF-β, MMPs expression and EMT. It has been demonstrated that TGF-β induces MMP-2 and MMP-9 expression by murine tubular epithelial cell lines [24,25]. Additionally, TGF-β1 induced MMP-mediated disruption of E-cadherin on tubular cells, which ultimately led to tubular cell EMT [26]. We have previously demonstrated that fibrotic kidneys of 2K1C rats have increased renal TGF-β1 expression compared to controls [12].

Interestingly, we demonstrated that MSCs transplantation reduced MMP-2 and MMP-9, while increased TIMP-1 and -2 in the clipped kidney of 2K1C rats to levels similar to those found in the Sham group. Furthermore, MSCs restored the renal basement membrane morphology and reduced myofibroblasts population in clipped kidneys of 2K1C rats. These results are consistent with *in vitro* and *in vivo* studies that evaluated the effect of MMPs inhibition on renal fibrosis. Mice with indirect reduction of MMP-9 activity or lacking MMP-9 gene showed a decreased disruption of tubular basement membrane along with a reduction in tubular cell EMT and fibrosis in kidneys injured by unilateral ureteral obstruction (UUO) [27,28], which also models the fibrotic scenario of CKD. Inhibition of MMP-2 activity mitigated TGF-β-induced tubular cell EMT, showing that MMP-2 is necessary for renal tubular EMT [29]. Inhibition of MMP-9 activity has also led to TGF-β-induced renal tubular cell EMT abrogation *in vitro* [25] and reduced interstitial myofibroblasts in UUO kidney [30]. Therefore, we postulate that MSCs normalize the expression of MMPs and its tissue inhibitors expression to levels that do not degrade renal basement membrane, allowing its restoration and, thereby mitigating the emergence of myofibroblasts from EMT.

We postulate that MSCs-derived TIMPs could have contributed to restoration of TIMP-1 and TIMP-2 expression in renal tissue. This hypothesis is supported by *in vitro* observations that bone marrow derived MSCs are capable to secrete TIMP-1 and -2, which were shown to protect the vascular environment from proteolytic disruption [31]. Moreover, the MSCs ability to secrete TIMP-1 is enhanced when cells are exposed to a pro-inflammatory or hypoxic environment [31,32], which is typical of the kidney fibrotic scenario.

In the present study we observed that damage by unilateral renal artery stenosis in 2K1C animals is accompanied not only by a significant increase of renal interstitial macrophages through the fibrotic parenchyma, but also by a marked increase in TNF-α expression, which was all blunted by MSCs transplantation. Accordingly, it was recently reported that MSCs reduced macrophages population in a CKD mice model of UUO [33,34]. However, different from the present study, MSCs therapy in UUO animals did not normalize the number of renal macrophages to levels present in the Sham group [33,34]. Distinct modes of pathological induction, time-point analysis, quantity of injected MSCs and its administration routes may account for the differences observed between studies. Arterially delivered MSCs attenuated TNF-α levels in

UUO animals [35]. Likewise, Oliveira-Sales and co-workers [13] observed that the increase of TNF-α mRNA expression in clipped kidneys of 2K1C rats was suppressed by MSCs treatment, which supports our findings in the present study regarding protein levels of TNF-α in kidneys before and after MSCs transplantation.

The decrease in TNF-α levels observed in clipped kidneys of 2K1C rats after cell therapy could be due to the reduction of the accumulation of macrophages, which are cells known to be able to secrete TNF-α when under a pro-inflammatory scenario [36,37]. TNF-α neutralization is associated to fibrosis amelioration and cell survival in UUO [38]. Therefore, the renoprotective effects of MSCs in 2K1C model of renal fibrosis reported in the present and previous studies by our group [12,13] may involve alterations in TNF-α production.

Our results demonstrated that partial occlusion of renal artery did not alter IL-10 levels, however MSCs delivery promoted a significant upregulation of this anti-inflammatory cytokine in 2K1C rats. Similar results were obtained when mRNA levels of IL-10 were analyzed in clipped kidneys of 2K1C rats [13]. Likewise, MSCs delivery into swine stenotic kidney also improved IL-10 expression [39]. Therefore, it could be postulated that this cytokine may participate in the MSC-induced renoprotective processes. Given the ability of MSCs to secrete IL-10 [40], they could be the source of IL-10 increase in treated 2K1C rats. Alternatively, MSCs may affect the remaining endogenous macrophages to increase their IL-10 production [41], thereby contributing to the increase of IL-10 in clipped kidneys of 2K1C animals. IL-10 expression was still high in clipped kidneys after two weeks of MSCs transplantation. This may have occurred because the injury inducer (renal artery partial occlusion) was persistent. It can be postulated that anti-inflammatory and regenerative processes mediated by IL-10 were possibly still in course. The mechanisms by which MSCs-mediated increase of IL-10 ameliorates renal tissue fibrosis should be explored in further studies.

Conclusion

In conclusion, we have shown that bone marrow-derived MSCs have a pleiotropic role in renal parenchyma remodeling of fibrotic kidneys from 2K1C rats by orchestrating anti-fibrotic and anti-inflammatory events that reversed renal fibrosis along with morphological restoration of renal parenchyma. Our study provides evidence of novel mechanisms by which MSCs reverse renal fibrosis in animals with renal artery stenosis, that is the control of balance between MMP-2/-9 and TIMP-1/2 expression. The reported effects of MSCs transplantation in 2K1C rats also involved the shift of a pro-inflammatory environment with TNF-α overexpression to an anti-inflammatory environment marked by IL-10 upregulation. These results contribute to an increasing understanding of how MSCs can be beneficial for renal fibrosis amelioration and tissue regeneration, supporting the notion that only one MSCs delivery into the renal subcapsular region represents a possible therapeutic strategy against renal fibrosis for CKD treatment.

Ethical approval

All applicable international, national, and/or institutional guidelines for the care and use of animals were followed. This article does not contain any studies with human participants performed by any of the authors.

Conflicts of interest

None.

REFERENCES

[1] Levey AS, Coresh J. Chronic kidney disease. Lancet 2012;379:165—80.
[2] Eddy AA. Progression in chronic kidney disease. Adv Chron Kidney Dis 2005;12:353—65.
[3] Nath KA. Tubulointerstitial changes as a major determinant in the progression of renal damage. Am J Kidney Dis 1992;20:1—17.
[4] Catania JM, Chen G, Parrish AR. Role of matrix metalloproteinases in renal pathophysiologies. Am J Physiol Ren Physiol 2007;292:F905—11.
[5] Cheng Z, Limbu MH, Wang Z, Liu J, Liu L, Zhang X, et al. MMP-2 and 9 in chronic kidney disease. Int J Mol Sci 2017;18:776.
[6] Ronco P, Lelongt B, Piedagnel R, Chatziantoniou C. Matrix metalloproteinases in kidney disease progression and repair: a case of flipping the coin. Semin Nephrol 2007;27:352—62.
[7] Conway B, Hughes J. Cellular orchestrators of renal fibrosis. QJM 2012;105:611—5.
[8] Djudjaj S, Boor P. Cellular and molecular mechanisms of kidney fibrosis. Mol Aspect Med 2019;65:16—36.
[9] Zhuang Q, Ma R, Yin Y, Lan T, Yu M, Ming Y. Mesenchymal stem cells in renal fibrosis: the flame of cytotherapy. Stem Cell Int 2019;2019:8387350.
[10] Shi M, Liu ZW, Wang FS. Immunomodulatory properties and therapeutic application of mesenchymal stem cells. Clin Exp Immunol 2011;164:1—8.
[11] Kyurkchiev D, Bochev I, Ivanova-Todorova E, Mourdjeva M, Oreshkova T, Belemezova K, et al. Secretion of

immunoregulatory cytokines by mesenchymal stem cells. World J Stem Cells 2014;6:552—70.

[12] Lira R, Oliveira M, Martins M, Silva C, Carvalho S, Stumbo AC, et al. Transplantation of bone marrow-derived MSCs improves renal function and Na$^+$+K$^+$-ATPase activity in rats with renovascular hypertension. Cell Tissue Res 2017;369:287—301.

[13] Oliveira-Sales EB, Maquigussa E, Semedo P, Pereira LG, Ferreira VM, Câmara NO, et al. Mesenchymal stem cells (MSC) prevented the progression of renovascular hypertension, improved renal function and architecture. PloS One 2013;8:e78464.

[14] Samadian F, Dalili N, Jamalian A. New insights into pathophysiology, diagnosis, and treatment of renovascular hypertension. Iran J Kidney Dis 2017;11:79—89.

[15] Labidi J, Touat D, Abdelghanim K, Ajili F, Ariba YB, Abdelhafidh NB, et al. Renovascular hypertension: a report of 21 cases. Saudi J Kidney Dis Transplant 2014;25:96—100.

[16] Oliveira M, Lira R, Freire T, Luna C, Martins M, Almeida A, et al. Bone marrow mononuclear cell transplantation rescues the glomerular filtration barrier and epithelial cellular junctions in a renovascular hypertension model. Exp Physiol 2019;104:740—54.

[17] Goldblatt H, Lynch J, Hanzal RF, Summerville WW. Studies on experimental hypertension I. The production of persistent elevation of systolic blood pressure by means of renal ischemia. J Exp Med 1934;59:347—79.

[18] Cavaglieri R, Martini D, Sogayar M, Noronha I. Mesenchymal stem cells delivered at the subcapsule of the kidney ameliorate renal disease in the rat remnant kidney model. Transplant Proc 2009;41:947—51.

[19] Cui R, Chen X, Peng L, Ma J, Zhu D, Li T, et al. Multiple mechanisms in renal artery stenosis-induced renal interstitial fibrosis. Nephron Exp Nephrol 2014;128:57—66.

[20] Warner GM, Cheng J, Knudsen BE, Gray CE, Deibel A, Juskewitch JE, et al. Genetic deficiency of Smad3 protects the kidneys from atrophy and interstitial fibrosis in 2K1C hypertension. Am J Physiol Ren Physiol 2012;302:F1455—64.

[21] LeBleu VS, Taduri G, O'Connell J, Teng Y, Cooke VG, Woda C, et al. Origin and function of myofibroblasts in kidney fibrosis. Nat Med 2013;19:1047—53.

[22] Gomez G, Velarde V. Boldine improves kidney damage in the Goldblatt 2K1C model avoiding the increase in TGF-b. Int J Mol Sci 2018;19:1864.

[23] Liu Y. Renal fibrosis: new insights into the pathogenesis and therapeutics. Kidney Int 2006;69:213—7.

[24] Strutz F, Zeisberg M, Ziyadeh FN, Yang CQ, Kalluri R, Müller GA, et al. Role of basic fibroblast growth factor-2 in epithelial-mesenchymal transformation. Kidney Int 2002;61:1714—28.

[25] Tan TK, Zheng G, Hsu TT, Wang Y, Lee VW, Tian X, et al. Macrophage matrix metalloproteinase-9 mediates epithelial-mesenchymal transition in vitro in murine renal tubular cells. Am J Pathol 2010;176:56—70.

[26] Zheng G, Lyons JG, Tan TK, Wang Y, Hsu TT, Min D, et al. Disruption of E-cadherin by matrix metalloproteinase directly mediates epithelial—mesenchymal transition downstream of transforming growth factor-beta1 in renal tubular epithelial cells. Am J Pathol 2009;175:580—91.

[27] Yang J, Shultz RW, Mars WM, Wegner RE, Li Y, Dai C, et al. Disruption of tissue-type plasminogen activator gene in mice reduces renal interstitial fibrosis in obstructive nephropathy. J Clin Invest 2002;110:1525—38.

[28] Wang X, Zhou Y, Tan R, Xiong M, He W, Fang L, et al. Mice lacking the matrix metalloproteinase-9 gene reduce renal interstitial fibrosis in obstructive nephropathy. Am J Physiol Ren Physiol 2010;299:F973—82.

[29] Cheng S, Lovett DH. Gelatinase A (MMP-2) is necessary and sufficient for renal tubular cell epithelial-mesenchymal transformation. Am J Pathol 2003;162:1937—49.

[30] Tan TK, Zheng G, Hsu TT, Lee SR, Zhang J, Zhao Y, et al. Matrix metalloproteinase-9 of tubular and macrophage origin contributes to the pathogenesis of renal fibrosis via macrophage recruitment through osteopontin cleavage. Lab Invest 2013;93:434—49.

[31] Lozito TP, Tuan RS. Mesenchymal stem cells inhibit both endogenous and exogenous MMPs via secreted TIMPs. J Cell Physiol 2011;226:385—96.

[32] Maffioli E, Nonnis S, Angioni R, Santagata F, Calì B, Zanotti L, et al. Proteomic analysis of the secretome of human bone marrow-derived mesenchymal stem cells primed by pro-inflammatory cytokines. J Proteomics 2017;166:115—26.

[33] Huuskes BM, Wise AF, Cox AJ, Lim EX, Payne NL, Kelly DJ, et al. Combination therapy of mesenchymal stem cells and serelaxin effectively attenuates renal fibrosis in obstructive nephropathy. FASEB J 2015;29:540—53.

[34] Xing L, Song E, Yu CY, Jia XB, Ma J, Sui MS, et al. Bone marrow-derived mesenchymal stem cells attenuate tubulointerstitial injury through multiple mechanisms in UUO model. J Cell Biochem 2019;120:9737—46.

[35] Asanuma H, Vanderbrink BA, Campbell MT, Hile KL, Zhang H, Meldrum DR, et al. Arterially delivered mesenchymal stem cells prevent obstruction-induced renal fibrosis. J Surg Res 2011;168:e51—9.

[36] Beutler BA. The role of tumor necrosis factor in health and disease. J Rheumatol Suppl 1999;57:16—21.

[37] Arango Duque G, Descoteaux A. Macrophage cytokines: involvement in immunity and infectious diseases. Front Immunol 2014;5:491.

[38] Meldrum KK, Misseri R, Metcalfe P, Dinarello CA, Hile KL, Meldrum DR. TNF-alpha neutralization ameliorates obstruction-induced renal fibrosis and dysfunction. Am J Physiol Regul Integr Comp Physiol 2007;292:R1456—64.

[39] Zhu XY, Urbieta-Caceres V, Krier JD, Textor SC, Lerman A, Lerman LO. Mesenchymal stem cells and endothelial progenitor cells decrease renal injury in experimental swine renal artery stenosis through different mechanisms. Stem Cells 2013;31:117—25.

[40] Aggarwal S, Pittenger MF. Human mesenchymal stem cells modulate allogeneic immune cell responses. Blood 2005;105:1815—22.

[41] Nemeth K, Leelahavanichkul A, Yuen PS, Mayer B, Parmelee A, Doi K, et al. Bone marrow stromal cells attenuate sepsis via prostaglandin E (2)-dependent reprogramming of host macrophages to increase their interleukin-10 production. Nat Med 2009;15:42—9.